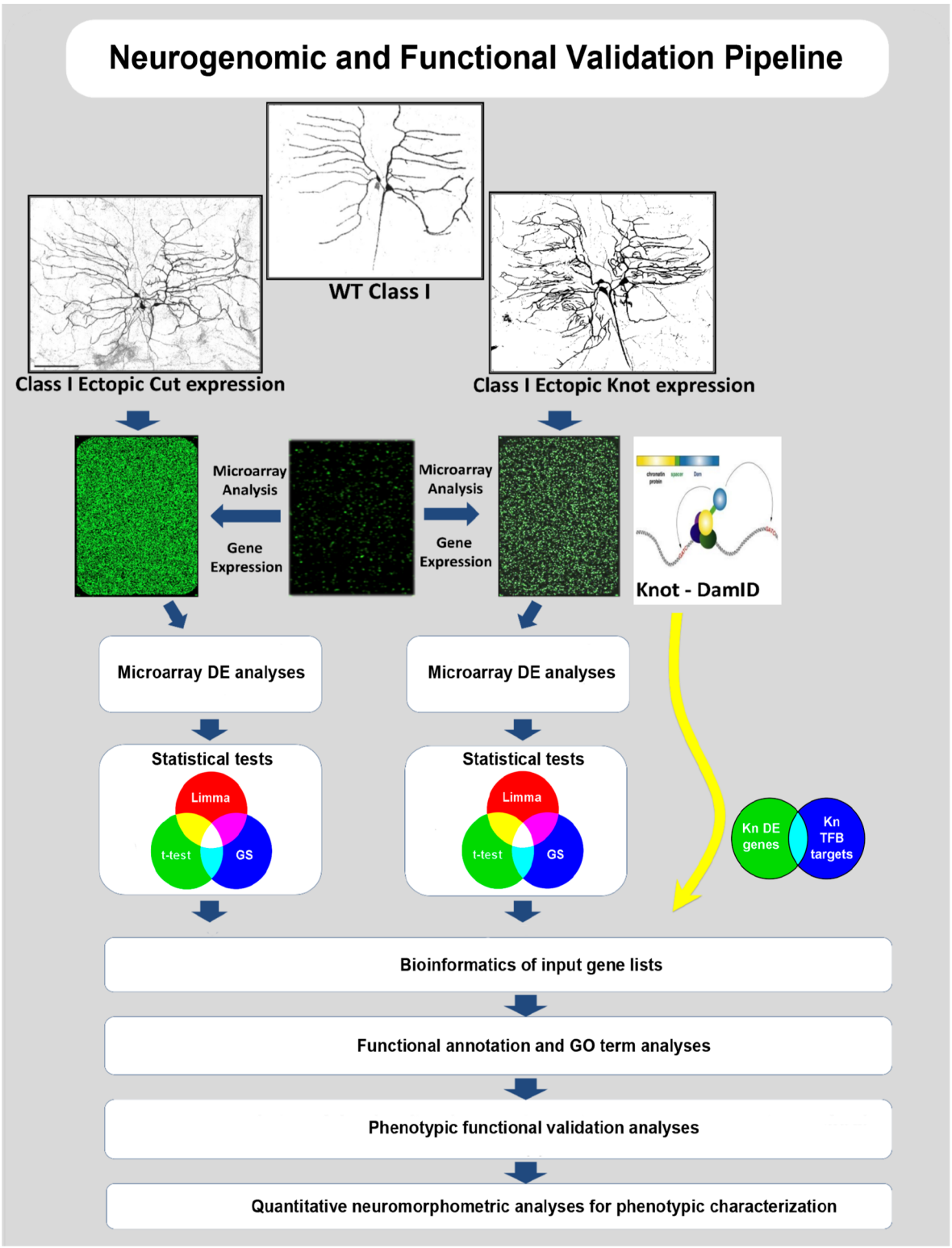

Figure S1. Neurogenomic dissection of Ct and Kn transcriptional effectors. Experimental outline of the neurogenomic strategy used in this study. The abbreviation used here are: WT (wild-type), Kn (Knot), DE (differential expression), TFB (transcription factor binding), Limma (Linear Models for Microarray Data), GS (GeneSpring), GO (Gene Ontology) and DAVID (The Database for Annotation, Visualization and Integrated Discovery).

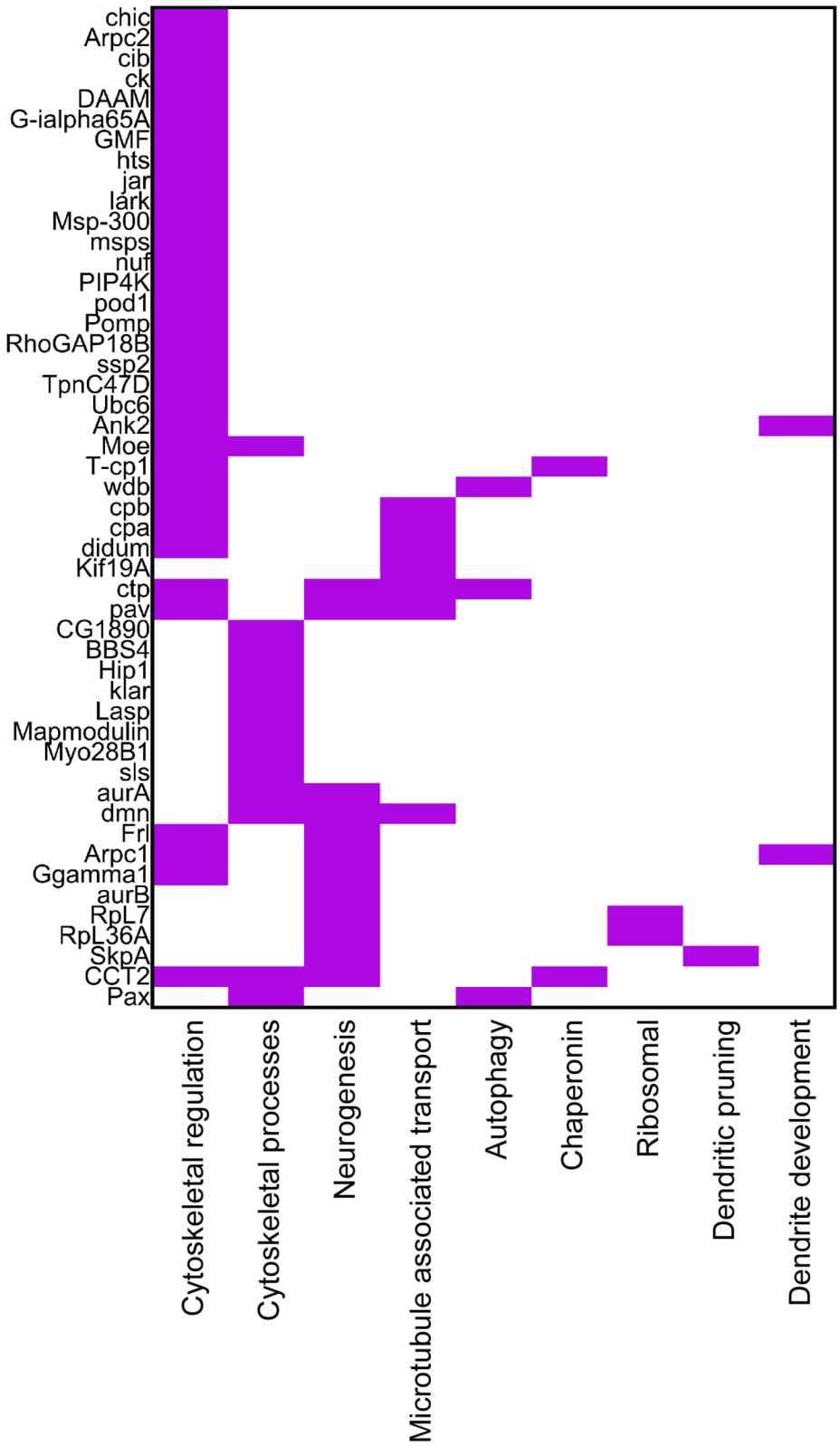

Figure S2. GO terms associated with candidate Ct/Kn targets. Visual matrix of major GO terms (x-axis) plotted against candidate targets from RNAi genetic screen (y-axis) reveals that select genes are associated with multiple GO terms, while others are linked to a distinct GO term.

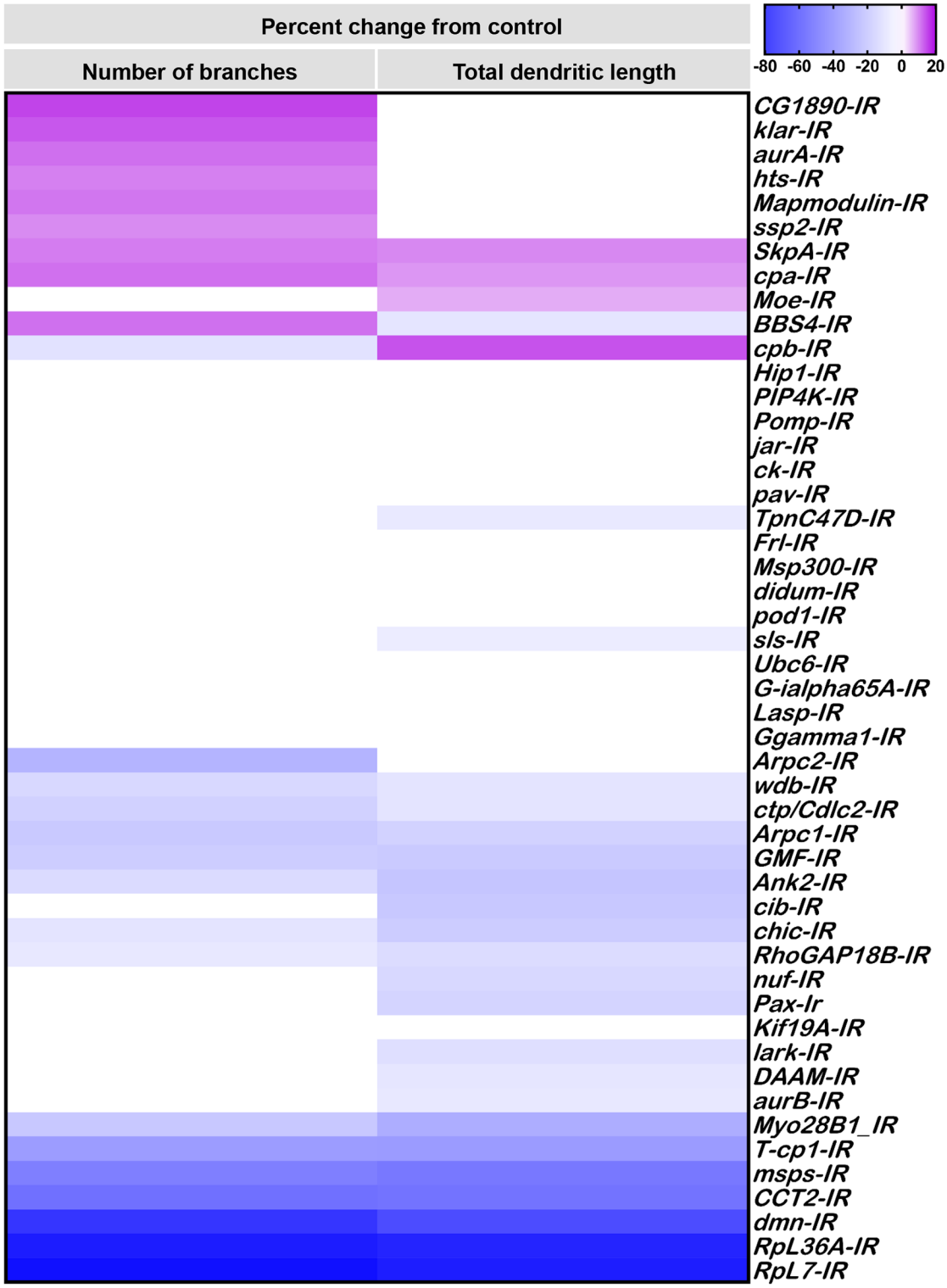

Figure S3. Phenotypic analyses of CIV dendritic architecture of all molecules screened.

Heatmap showing percentage change in number of branches (left column) and total dendritic length (right column) as compared to control. Negative change indicates a reduction and positive change indicate an increase of that morphological feature relative to control. All the non-significant scores were normalized to “0” for simplicity, all the non-white shells were significant with $p<0.05$; N=7-12 neurons; multiple t-tests.

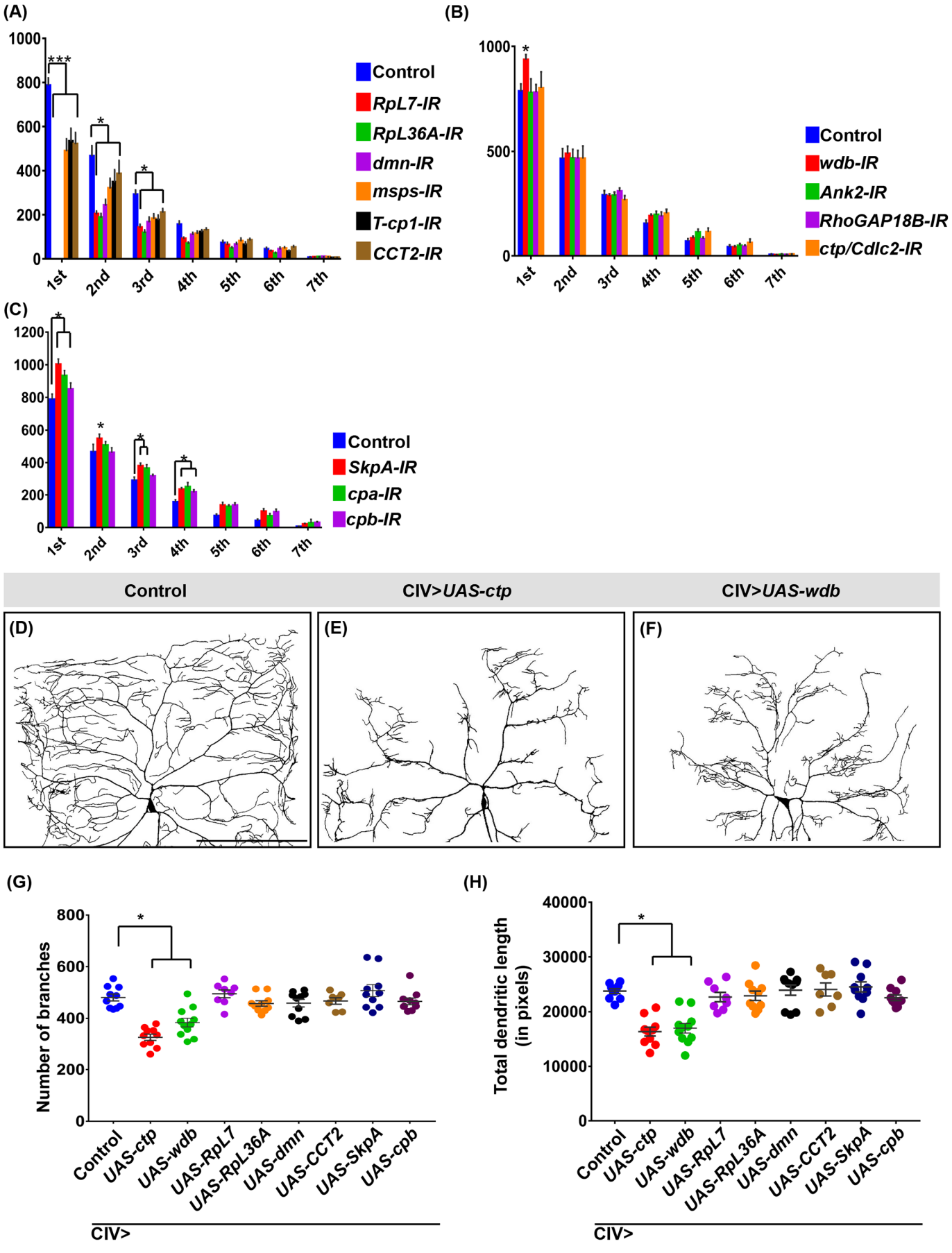
(A)
1000
800
600
400
200
0
***
*
*
1st
2nd
3rd
4th
5th
6th
7th
Control
RpL7-IR
RpL36A-IR
dmn-IR
msps-IR
T-cp1-IR
CCT2-IR
(B)
1000
500
0
*
1st
2nd
3rd
4th
5th
6th
7th
Control
wdb-IR
Ank2-IR
RhoGAP18B-IR
ctp/Cdlc2-IR
(C)
1200
1000
800
600
400
200
0
*
*
*
*
1st
2nd
3rd
4th
5th
6th
7th
Control
SkpA-IR
cpa-IR
cpb-IR
Control
CIV>UAS-ctp
CIV>UAS-wdb
(D)
(E)
(F)
(G)
Number of branches
800
600
400
200
0
*
Control
UAS-ctp
UAS-wdb
UAS-RpL7
UAS-RpL36A
UAS-dmn
UAS-CCT2
UAS-SkpA
UAS-cpb
CIV>
(H)
Total dendritic length (in pixels)
40000
30000
20000
10000
0
*
Control
UAS-ctp
UAS-wdb
UAS-RpL7
UAS-RpL36A
UAS-dmn
UAS-CCT2
UAS-SkpA
UAS-cpb
CIV>

Figure S4. Strahler order and overexpression analyses of putative Ct/Kn effector genes. (**A-C**) Strahler order analyses of branch order distribution of the gene-specific IR knockdowns in the complexity enhancer (**A**), complexity shifter (**B**) and complexity suppressor (**C**) categories. The values are the mean (±SEM) for the number of dendritic branches in each branch order, where 7 =primary branch from cell body and 1=terminal branches. (**D-F**) Representative images of CIV (ddaC) neuron dendritic arborization in control and overexpression of the corresponding genes. (**G,H**) Quantitative analyses measuring number of branches (**G**) and total dendritic length (**H**) Statistical tests performed, (**A-C**) two-way ANOVA with FDR correction of Benjamini, Kriega and Yekutieli, N=7-10 neurons. (**G,H**) one-way ANOVA with FDR correction of Benjamini, Kriega and Yekutieli, N= 7-11 neurons. Significance scores are *=$p < 0.05$ and ***= $p < 0.001$. Scale bar 200 μm.

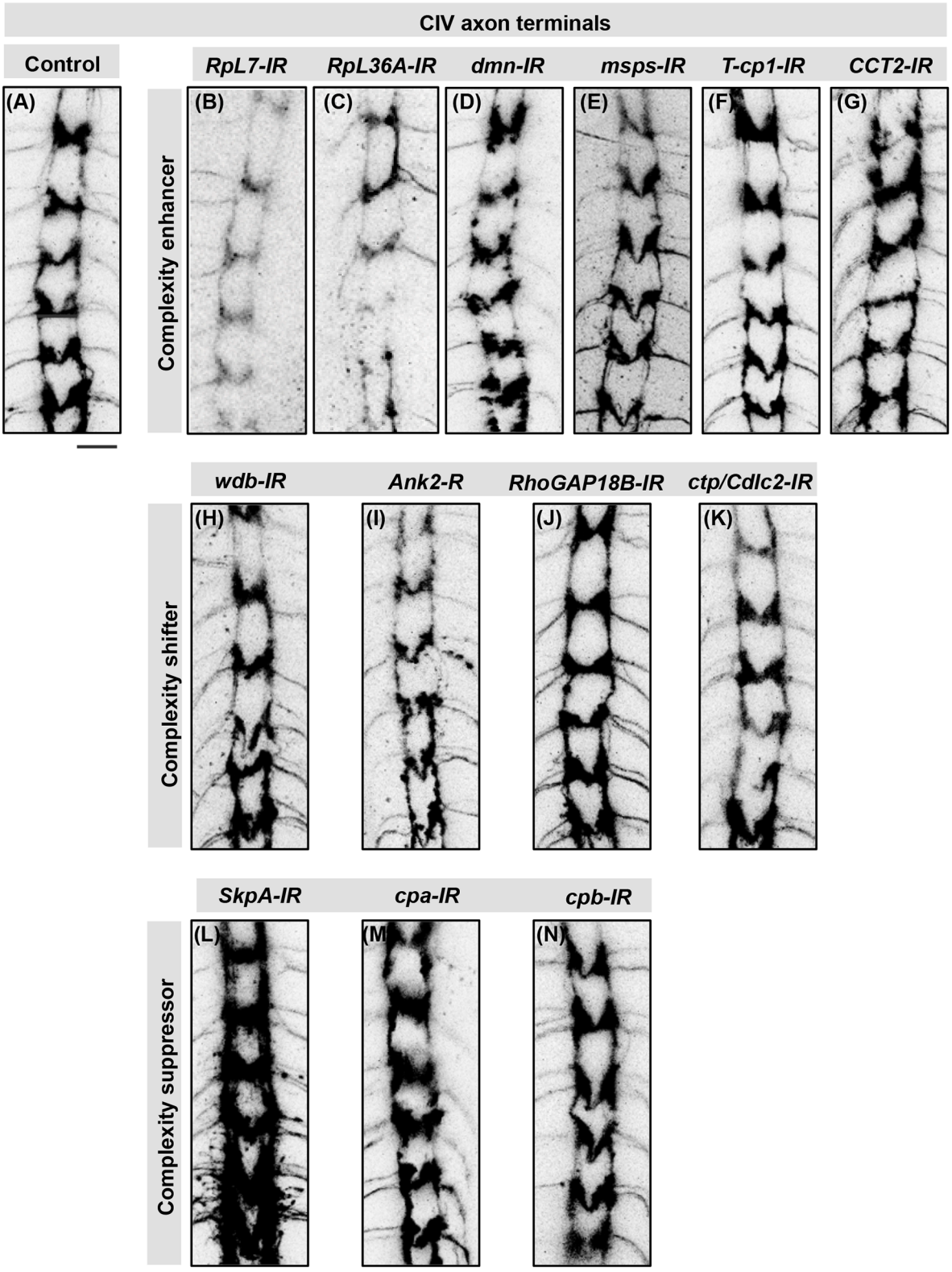

Figure S5. CIV axonal patterning of putative Ct/Kn effector molecules
Representative images of CIV da neuron axon terminals in the VNC labeled with *GAL4[477]; ppk-CD4::tdTomato* (L3 larvae). (**A**) Control, and the genes that fall in (**B-G**) complexity enhancer category; (**H-K**) complexity shifter category; (**L-N**) complexity suppressor category. Scale bar is 20 μm.

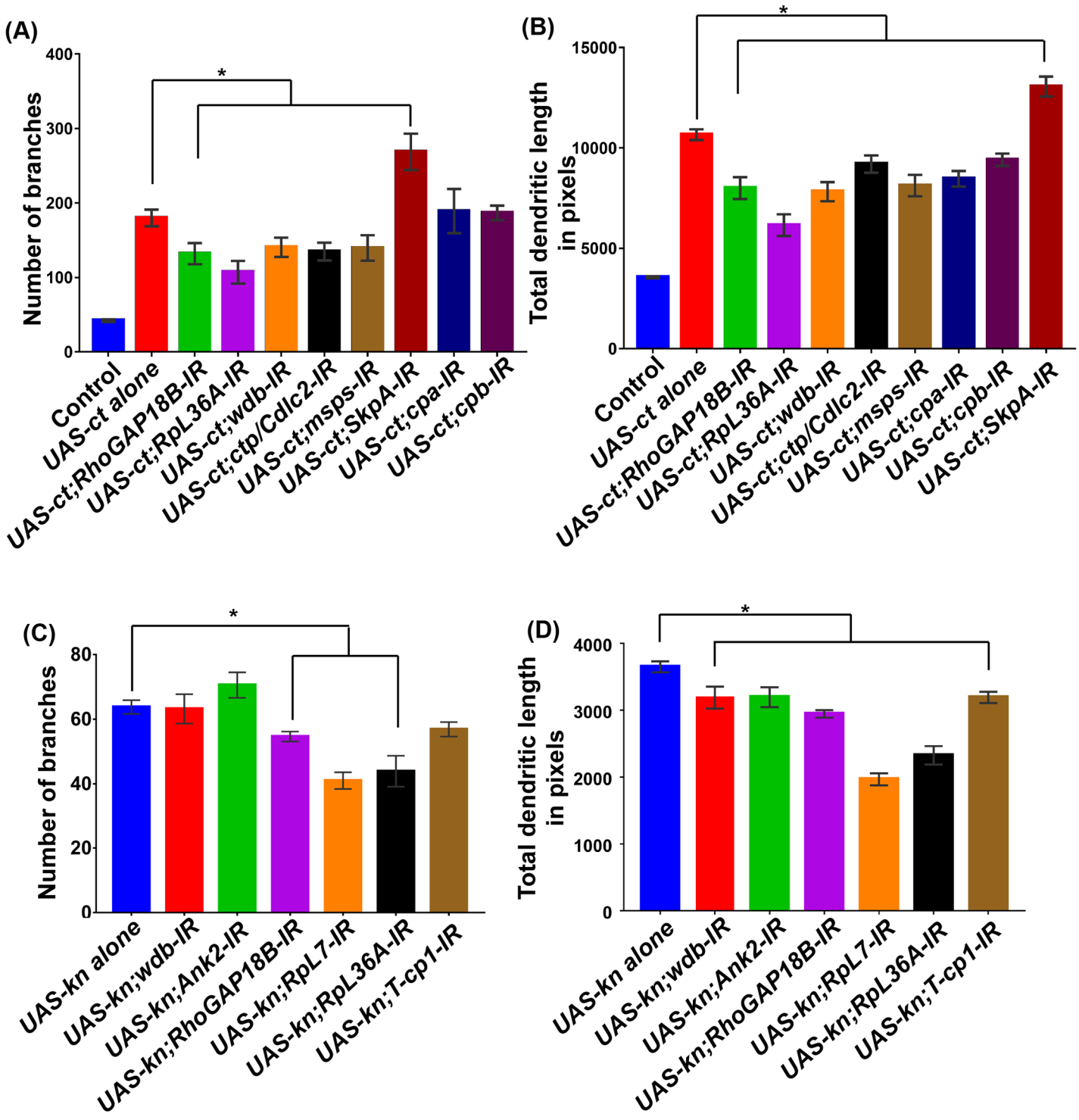

Figure S6. Quantitative enhancer/suppressor analyses of putative Ct and Kn effector molecules.

Quantitative neuromorphometric analyses CI vpda neurons overexpressing Ct with simultaneous RNAi (IR) knockdown of Ct candidate target genes (**A,B**), and CI vpda neurons overexpressing Kn with simultaneous RNAi knockdown of Kn candidate target genes (**C,D**). Statistical test performed in **(A-D)**: one-way ANOVA with FDR correction of Benjamini, Kriega and Yekutieli N=7-15 neurons, and significance scores were *=$p < 0.05$.

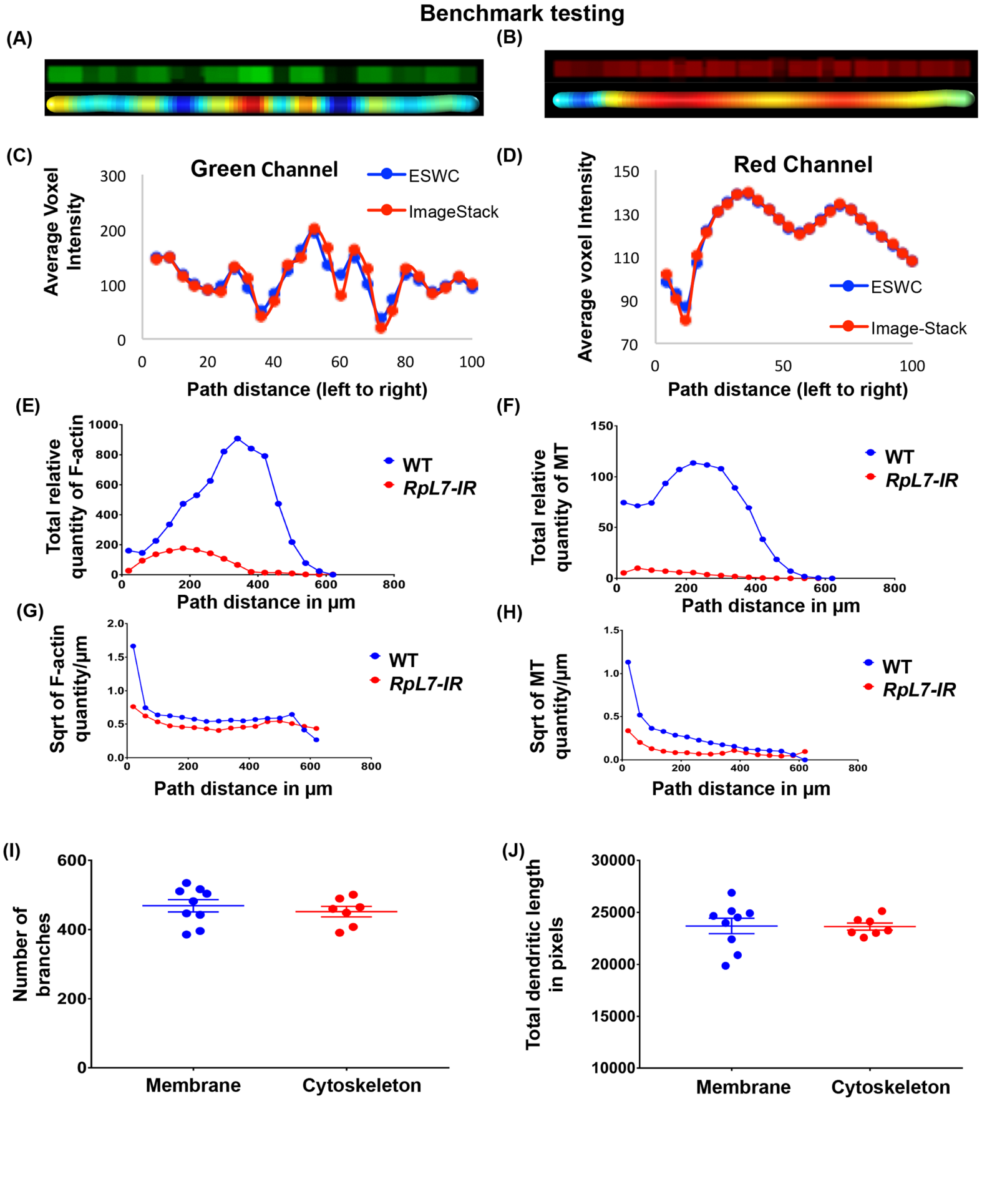
Benchmark testing
(A)
(B)
(C)
Green Channel
ESWC
ImageStack
Average Voxel Intensity
Path distance (left to right)
(D)
Red Channel
Average voxel Intensity
ESWC
Image-Stack
Path distance (left to right)
(E)
Total relative quantity of F-actin
WT
RpL7-IR
Path distance in µm
(F)
Total relative quantity of MT
WT
RpL7-IR
Path distance in µm
(G)
Sqrt of F-actin quantity/µm
WT
RpL7-IR
Path distance in µm
(H)
Sqrt of MT quantity/µm
WT
RpL7-IR
Path distance in µm
(I)
Number of branches
Membrane
Cytoskeleton
(J)
Total dendritic length in pixels
Membrane
Cytoskeleton

Figure S7. Benchmark analyses of multichannel reconstructions and reporters. (**A,B**) Artificial image stack of a surrogate dendritic branch (cylinder) with arbitrary intensity values (0 to 255) assigned to all voxels for a green channel (representing F-actin, **A**) and a red channel (representing MTs, **B**). The voxels in the artificial image stack are isotropic in shape (1 micron in each of the three dimensions) and the overall image stack dimensions are 512 x 512 x 7 with a length of 100 microns and radius of 2.5 microns for the surrogate cylinder. Presented below each artificial image channel is the look up table (LUT) representing signal intensities from low (blue) to high (red) across the cylinder. (**C,D**) The artificial dendritic cylinder is then traced and a ESWC file is generated using the Vaa3D multichannel plugin. Comparisons of average voxel intensity distribution (against path distance) of the generated ESWC files against known distributions of the artificially generated surrogate dendritic cylinder (for both the green/F-actin (**C**) and the red/microtubule channels (**D**)) reveal the Vaa3D multichannel plug-in accurately measures voxel intensities resulting from the artificial image stack. (**E,F**) Representative plots depicting changes in total relative quantities of F-actin (**E**) or MT (**F**) within a 40 micron bin as a function of path distance in microns from the soma for control (WT) vs. RpL7-IR CIV neurons. (**G,H**) Representative plots depicting average relative quantities of F-actin (**G**) or MT (**H**) for WT vs. RpL7-IR CIV neurons normalized to length (square root (sqrt) quantity per micrometer dendrite). (**I, J**) Neuromorphometric comparisons of the mean ± SEM for the number of dendritic branches (**I**) and total dendritic length (**J**) between CIV neurons labeled with a CD8::GFP tagged membrane reporter vs. the multi-fluor cytoskeletal reporter (GFP/F-actin; mCherry/MT) reveal no significant differences (N=7-9 neurons). Statistics: unpaired t-test.

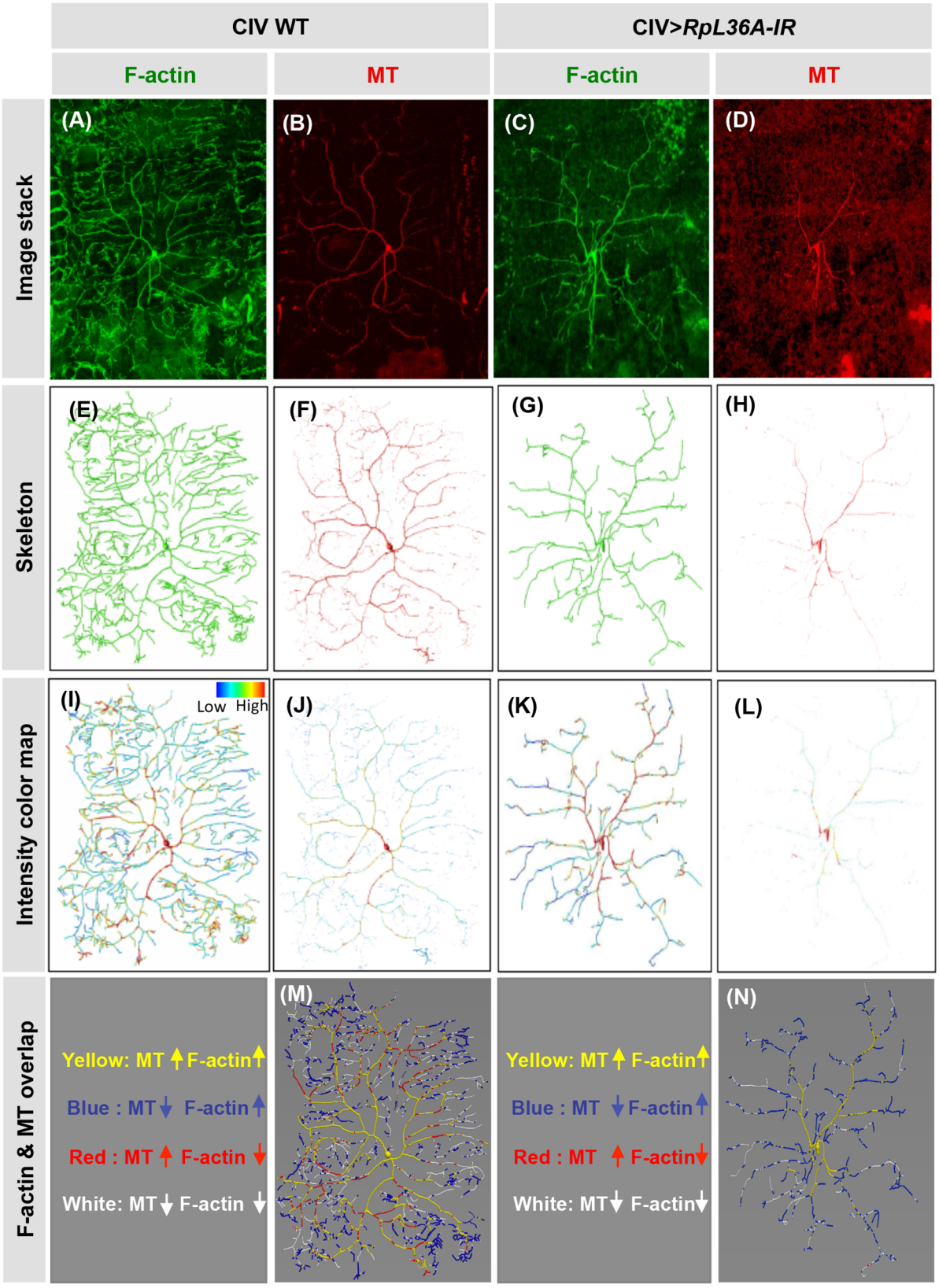

Figure S8. Multichannel reconstructions enable detailed analyses of both global and local changes in dendritic cytoskeletal *organization.*
(A-D) Representative multi-fluor cytoskeletal reporters images of the individual channels of WT and *RpL36A-IR* CIV neurons. **(E-H)** Skeletons of the reconstructions generated by a combination of Vaa3D, Neutube and TREES Toolbox. **(I-L)** Intensity maps of F-actin and MT generated in Vaa3D. **(M, N)** Relative subcellular distributions of F-actin and MTs.